





# **Data, Innovation, and Science Cluster**

# Description of the Processing Algorithms

Delft University of Technology (DUT)
Centre National D'Études Spatial (CNES)
Deutsches Zentrum für Luft- und Raumfahrt (DLR)
Rheinische Friedrich-Wilhelms-Universität Bonn (GFZ)

Doc. no.: SW-TN-DUT-GS-129_03	3
-------------------------------	---

Rev.: 0

Prepared:		Checked:	
Christian Siemes	Date 2022-07-07	Christian Siemes	Date 2022-07-07
Team Leader		Team Leader	
Approved:			
Christian Siemes	Date 2022-07-07		
Team Leader			





DISC SW-TN-DUT-GS-129\_03 Revision 1

Page 2 of 10

**Description of the Processing Algorithms** 

### **Record of Changes**

Reason	Description	Rev	Date
Initial version	Released	0	2021-07-07
Revision 1	Clarified in Section 1.1 that new algorithms in the processing will be explained in a scientific publication	1	2022-09-09





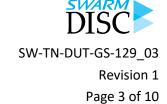


#### **Table of Contents**

1	Intr	oduction	4
	1.1	Scope	4
2	Арр	olicable and Reference Documentation	5
	2.1	Applicable Documents	5
	2.2	Reference Documents	5
	2.3	Abbreviations	6
3	Pro	cessing of density and crosswind observations	7
	3.1	Accelerometer data preprocessing	8
	3.2	Accelerometer data calibration	8
	3.3	Satellite radiation pressure model	8
	3.4	Satellite aerodynamic model	8
	3.5	Density and crosswind retrieval	9





DISC
SW-TN-DUT-GS-129\_03
Revision 1
Page 4 of 10

**Description of the Processing Algorithms** 

#### 1 Introduction

#### 1.1 Scope

This document describes the processing algorithms that lead to the data products that are produced within the TOLEOS project in agreement with the requirements specified in [AD-1].

The processing from raw accelerometer measurements to thermosphere density and crosswind observations is very complex. Therefore, this document will only provide a high-level overview of the processing and refer to the relevant scientific publications for the existing algorithms. The new elements of the processing algorithms will be described in a dedicated scientific publication that is currently in preparation. The tentative title is "New thermosphere neutral density and crosswind datasets from CHAMP, GRACE, and GRACE-FO". We intend to submit the manuscript to the "Journal of Space Weather and Space Climate".







## 2 Applicable and Reference Documentation

#### 2.1 Applicable Documents

The following documents are applicable to the definitions within this document.

[AD-1] TOLEOS – Thermosphere Observations from Low-Earth Orbiting Satellites. Proposal for Swarm DISC ITT 4.3, SW-OF-DUT-GS-129, Revision 1

#### 2.2 Reference Documents

The following documents contain supporting and background information to be taken into account during the activities specified within this document.

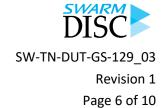
[RD-1] Doornbos, E. (2011) Thermosphere density and wind determination from satellite dynamics. Dissertation, Delft University of Technology. http://resolver.tudelft.nl/uuid:33002be1-1498-4bec-a440-4c90ec149aea [RD-2] Montenbruck, O., Gill, E. (2012) Satellite orbits – Models, Methods Applications (1st ed.). Springer. http://doi.org/10.1007/978-3-642-58351-3 [RD-3] March, G., Doornbos, E. & Visser, P., 2019a. High-fidelity geometry models for improving the consistency of CHAMP, GRACE, GOCE and Swarm thermospheric density data sets. Advances in Space Research, 63: 213–238. https://doi.org/10.1016/j.asr.2018.07.009 [RD-4] March, G., Visser, T., Visser, P., Doornbos, E., 2019b. CHAMP and GOCE thermospheric wind characterization with improved gas-surface interactions modelling. Advances in Space Research, 64: 1225–1242. https://doi.org/10.1016/j.asr.2019.06.023 [RD-5] March, G., van den IJssel, J., Siemes, C., Visser, P., Doornbos, E., Pilinski, M. (2021) Gassurface interactions modelling influence on satellite aerodynamics and thermosphere mass density. J. Space Weather Space Clim., https://doi.org/10.1051/swsc/2021035 [RD-6] Sentman, L., 1961. Free molecule flow theory and its application to the determination of aerodynamic forces, Sunnyvale, California, US: LMSC-448514, Lockheed Missiles Space Company. Van Helleputte, T., Doornbos, E. & Visser, P., 2009. CHAMP and GRACE accelerometer [RD-7] calibration by GPS-based orbit determination. Advances in Space Research, 43: 1890-1896. https://doi.org/10.1016/j.asr.2009.02.017 [RD-8] Wöske, F., Kato, T., Rievers, B., List, M., 2019. GRACE accelerometer calibration by high

1335. https://doi.org/10.1016/j.asr.2018.10.025

precision non-gravitational force modelling. Advances in Space Research 63 (2019) 1318-







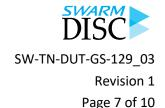
### 2.3 Abbreviations

The following list defines the acronyms used within this document.

Acronym	Description
AOCS	Attitude and Orbit Control System
CAD	Computer-Aided Design
CHAMP	Challenging Mini-satellite Payload
DSMC	Direct Simulation Monte Carlo
GNSS	Global Navigation Satellite System
GRACE	Gravity Recovery and Climate Experiment
GRACE-FO	Gravity Recovery and Climate Experiment Follow-On
LTAN	Local Time of the Ascending Node
NRTDM	Near Real-Time Density Modelling
SPARTA	Stochastic Parallel Rarefied-Gas Time-Accurate Analyzer
TOLEOS	Thermosphere Observations from Low-Earth Orbiting Satellites

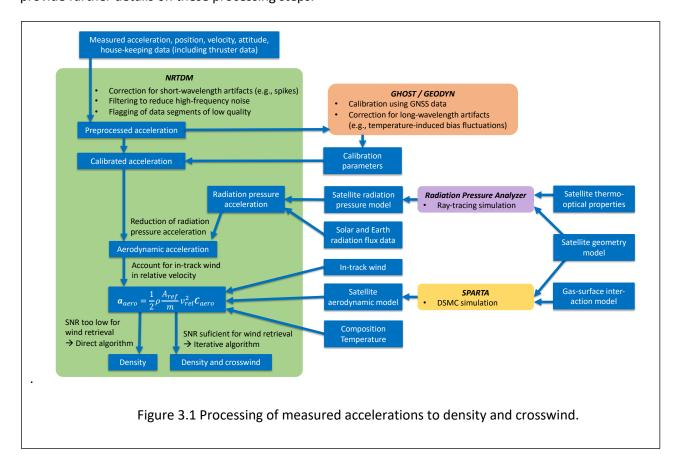






## 3 Processing of density and crosswind observations

The processing of acceleration measurements to density and crosswind observations is well-established. An instructive and complete description is available in [RD-1] and an overview is provided in Figure 3.1. Starting from the measured acceleration, the first step is the preprocessing that reduces any kind of undesired signal and noise to obtain a "clean" acceleration. These accelerations are still scaled and biased. Therefore, the next step is the estimation of the scale and bias parameters in a precise orbit determination approach using GNSS receiver data and, subsequently, apply these parameters to obtain the calibrated acceleration. The aerodynamic acceleration  $\mathbf{a}_{aero}$  is obtained by subtracting the radiation pressure acceleration from the calibrated one. The radiation pressure is modelled on the basis of solar and Earth radiation flux data in combination with a satellite model for radiation pressure. The latter is determined via a ray tracing simulation. In a similar way, we obtain an aerodynamic satellite model via a DSMC simulation of aerodynamic forces. This model is essentially a lookup table for the aerodynamic coefficient vector  $\mathbf{c}_{aero}$ . Once both the aerodynamic acceleration and the aerodynamic satellite model are available, the density and crosswind observations are derived via direct and iterative algorithms as described in [RD-1]. The following sections provide further details on these processing steps.







DISC
SW-TN-DUT-GS-129\_03
Revision 1
Page 8 of 10

**Description of the Processing Algorithms** 

#### 3.1 Accelerometer data preprocessing

The accelerometer preprocessing aims at reducing all kinds of undesired signals and noise. This includes in particular artificial spikes, thermally induced bias variations (in case of the GRACE mission), and accelerations due to thruster activations. Spikes are typically detected by applying a moving-median filter to the accelerometer measurements and detecting outliers in the residuals. In addition, house-keeping data from the AOCS is used to identify thruster activations, whose (residual) acceleration signal is subsequently removed from the data. It is worth mentioning that the preprocessing performed in the TOLEOS project is tailored to the specifics of the accelerometer measurements from each mission.

#### 3.2 Accelerometer data calibration

The estimation of calibration parameter is described in detail in [RD-7]. In short, the calibrated accelerations are expressed as a linear function of the preprocessed acceleration, where a scale factor and a bias are the parameters of the linear function. These parameters are adjusted within a precise orbit determination procedure, where the sum of gravitational and non-gravitational accelerations is integrated twice and fitted to a precise orbit that was derived from the GNSS receiver data.

## 3.3 High-fidelity satellite geometry model

The satellite geometry models form the basis for the radiation pressure and aerodynamic modelling. High-fidelity geometry models were already available for the CHAMP and GRACE satellites as described in [RD-3]. For the GRACE-FO satellite, we derived the high-fidelity geometry model directly from the CAD model of the satellites using the Blender software. The derivation requires to reduce the CAD model to the outer surface, which is required to be "water-tight". Further, the surface is simplified to some extent to reduce the number of facets, which facilitates a reasonable run-time of the radiation pressure and aerodynamic simulations.

#### 3.4 Satellite radiation pressure model

The satellite radiation pressure model has two components. The first is the radiation pressure force coefficient vector that is determined within a ray tracing simulation. In short, simulated light rays are traced to surface elements of the satellite geometry, where they create a pressure on the surface that depends on the absorptive and reflective properties of the surface. This allows to account for shadowing and multiple reflections. The second component of the radiation pressure model is a thermal model of the satellite, which is very similar to the one described by [RD-8]. The advantage of this model is that we can integrate the absorbed radiation along the orbit and, thus, account for the thermal inertia of the satellite.

#### 3.5 Satellite aerodynamic model

The satellite aerodynamic model is described in depth in [RD-3], [RD-4], and [RD-5]. It obtained via a DSMC simulation where the gas-surface interaction is assumed to be diffuse with incomplete energy





DISC
SW-TN-DUT-GS-129\_03
Revision 1
Page 9 of 10

**Description of the Processing Algorithms** 

accommodation, which follows from [RD-6]. The aerodynamic models for the CHAMP and GRACE satellites were already available from [RD-5]. The aerodynamic model for the GRACE-FO satellites was obtained in the same way as describe in Section 3.3.

### 3.6 Density and crosswind retrieval

The density and crosswind observations are derived by the direct and iterative algorithms described in detail in [RD-1]. For the density observations, we always use the direct algorithm where the acceleration is projected onto the x-axis of the satellite reference frame, which is approximately aligned with the flight direction. This guarantees a large aerodynamic signal in the nominal flight orientation and guarantees that only the sensitive accelerometer axis is used, which is also the most accurate in terms of calibration. The crosswind observations are obtained using the iterative algorithm since this algorithm.





DISC
SW-TN-DUT-GS-129\_03
Revision 1
Page 10 of 10

**Description of the Processing Algorithms** 

## 4 Processing of conjunctions

The conjunctions that we consider are crossovers that occur in fast succession and alignments of the orbital planes. In Sections 4.1 and 4.2 we outline the algorithms for the detection of these types of conjunctions. It should be noted that both crossovers and plane alignments are detected purely on the basis of the orbits, i.e. irrespective of the availability of the density and crosswind observations.

#### 4.1 Crossovers

Crossovers are defined as the location where the ground tracks cross, where the location is expressed in geodetic latitude and longitude. This includes crossovers of the ground track with itself, which occur after one orbital revolution. We calculate also the time differences between the first and second satellite passing over the same location and omit all crossovers for which the time difference exceeds a predefined threshold. The algorithm to find crossovers is a simple line intersection method, where the only complications arise from data gaps and the fact that a ground track may pass over the east-west boundary of the map.

#### 4.2 Orbital plane alignments

We define orbital plane alignments as those epochs, where the LTAN of the first satellite's orbit is identical to that of the second satellite's orbit. The calculation of the LTAN is described in [RD-2]. In practice, we calculate the LTAN as time series and check at which epochs two LTAN time series intersect using again a simple line intersection method. The only complications are data gaps, the cyclic nature of the LTAN (range 0-24 hours), and the fact that we detect both rotating and counter-rotating orbits, i.e. 24 and 12 hours LTAN differences, respectively.